Journal of Sound and Vibration (1996) **198**(5), 643–650

STABILITY OF A PARAMETRICALLY EXCITED DAMPED INVERTED PENDULUM

G. Erdos and T. Singh

Department of Mechanical and Aerospace Engineering, SUNY at Buffalo, Buffalo, NY 14260, U.S.A.

(*Received* 3 *November* 1995, *and in final form* 28 *March* 1996)

1. INTRODUCTION

The transition of stability of the vertically upright position of the pendulum from an unstable to a stable configuration has been illustrated in the literature when the pivot of the pendulum is subject to a periodic motion. Many studies, which have included analytical and numerical approaches, have been used to determine the conditions for stability. The stability border has been calculated for the undamped case by Landau and Lifshitz [2] using the averaging method. Other analytical tools, such as the method of small parameters by Hsu [6], and the harmonic balance method by Clifford and Bishop [3], have been used to determine the stability border. A numerical approach was utilized by Capecchi and Bishop [4] to arrive at the stability border. Arnold [7] provides an elegant stability condition for *uncompressible flows* using the trace of the Poincaré map (or monodromy matrix). In this note we use the Floquet theory and variational system to calculate the stability border in closed form. An overview of the mathematical tools that are used to calculate the stability border are provided. We then compute the stability border in the viscous damped case, using the same tools as in the undamped case.

2. PARAMETRICALLY EXCITED UNDAMPED INVERTED PENDULUM

In this section the stability of an undamped inverted pendulum is considered. The pivot point of a simple inverted pendulum (Figure 1) is subjected to vertical oscillation of the form $y(t) = \varepsilon \cos(\omega t)$. Our goal here is to establish the stability border that relates the amplitude (ε) to the frequency (ω) of the forcing function. The equation of motion of the inverted pendulum is

$$\ddot{x} = \left(\frac{g}{l} - \frac{\varepsilon\omega^2}{l}\cos(\omega t)\right)\sin(x), \tag{1}$$

where g is the acceleration due to gravity and l is the length of the pendulum. Since we are interested in the stability of the vertically upright position of the pendulum, we linearize equation (1) around $x = 0$, leading to

$$\ddot{x} = \left(\frac{g}{l} - \frac{\varepsilon\omega^2}{l}\cos(\omega t)\right)x. \tag{2}$$

0022–460X/96/500643 + 08 $25.00/0

Equation (2) can be represented in state space form as

$$\begin{pmatrix}\dot{x}_1\\ \dot{x}_2\end{pmatrix} = \begin{bmatrix} 0 & 1\\ \dfrac{g}{l} - \dfrac{\varepsilon\omega^2}{l}\cos(\omega t) & 0\end{bmatrix}\begin{pmatrix}x_1\\ x_2\end{pmatrix}. \tag{3}$$

Equation (3) has the same form as the equation

$$\dot{\mathbf{x}} = A(t)\mathbf{x}, \qquad x \in \Re^n, \quad A(t+p) = A(t), \tag{4}$$

with a period $p = 2\pi/\omega$. The stability of the upright position depends on the characteristic roots of the *period-advance* map $M = g_0^p$ [7]. The characteristic roots σ_1 and σ_2 satisfy the characteristic equation of the matrix M, which are given by the equation

$$\sigma^2 - \mathrm{Tr}\,(M)\sigma + \mathrm{Det}\,(M) = 0, \tag{5}$$

where

$$\mathrm{Det}\,(M) = \mathrm{e}^{\int_0^p \mathrm{Tr}(A(\tau))\,\mathrm{d}\tau} \qquad \mathrm{Tr}\,(M) = \mathrm{Tr}\,(g_0^p). \tag{6,7}$$

From equations (6), (7) and (3), it follows that $\mathrm{Det}\,(M) = \mathrm{e}^{\int_0^p 0\,\mathrm{d}\tau} = 1$: therefore

$$\sigma^2 - \mathrm{Tr}\,(M)\sigma + 1 = 0. \tag{8}$$

The roots of equation (8) are

$$\sigma_{1,2} = \frac{\mathrm{Tr}\,(M) \pm \sqrt{\mathrm{Tr}^2\,(M) - 4}}{2} \tag{9}$$

If $\mathrm{abs}\,(\mathrm{Tr}\,(M)) > 2$, then roots of equation (8) are real and

$$\mathrm{abs}\,(\mathrm{Tr}\,(M)) = \mathrm{abs}\,(\sigma_1 + \sigma_2) > 2. \tag{10}$$

Since the *characteristic multipliers* of $A(t)$ have to lie within the unit circle, we require $|\sigma_{1,2}| \leqslant 1$ [7]. This requirement conflicts with equation (10), as the sum of the two roots is greater than 2. Therefore, for stability, we require

$$\mathrm{abs}\,(\mathrm{Tr}\,(M)) = \mathrm{abs}\,(\sigma_1 + \sigma_2) \leqslant 2. \tag{11}$$

The stability border is given by the equation

$$|\mathrm{Tr}\,(M)| = 2. \tag{12}$$

Determination of the stability border requires a closed form solution of equation (3), which is not available. However, if the amplitude of the excitation (ε) is small, we can approximate the solution of equation (3) by expanding it into a Taylor series with respect

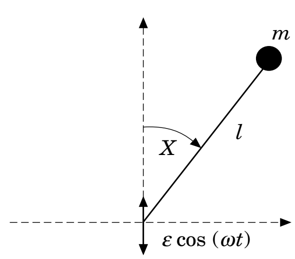

Figure 1. A vertically excited inverted pendulum.

to ε around $\varepsilon = 0$. Since the right side of equation (3) is a smooth function ε, the solution is differentiable with respect to ε [9]. The solution $\xi(t)$ can be approximated as follows:

$$\boldsymbol{\xi}(t, \varepsilon) = \mathbf{x}(t, 0) + \mathbf{y}(t, 0)\varepsilon + \tfrac{1}{2}\mathbf{z}(t, 0)\varepsilon^2 + o(\varepsilon^3), \tag{13}$$

where $\mathbf{x}(t, 0) = \boldsymbol{\xi}(t, 0)$, $\mathbf{y}(t, 0) = (\partial\boldsymbol{\xi}(t, \varepsilon/\partial\varepsilon)/_{\varepsilon=0}$ and $\mathbf{z}(t, 0) = \partial^2\boldsymbol{\xi}(t, \varepsilon)/\partial\varepsilon^2)/_{\varepsilon=0}$.

To calculate the M matrix we have to obtain the fundamental matrix of equation (3). The column vectors of the fundamental matrix are two linearly independent solutions of equation (3). Since equation (3) is linear, if the initial values are linearly independent, the corresponding solutions are linearly independent. We choose [1, 0] and [0, 1] as the set of initial values to calculate two independent solutions $\xi^{1,0}(t, \varepsilon)$ and $\xi^{0,1}(t, \varepsilon)$ of equation (3):

$$\begin{pmatrix} \dot{\xi}_1 \\ \dot{\xi}_2 \end{pmatrix} = A(t, \varepsilon)\begin{pmatrix} \xi_1 \\ \xi_2 \end{pmatrix} \qquad \text{where} \quad A(t, \varepsilon) = \begin{bmatrix} 0 & 1 \\ \dfrac{g}{l} - \dfrac{\varepsilon\omega^2}{l}\cos(\omega t) & 0 \end{bmatrix},$$

$$\begin{pmatrix} \xi_1(0) \\ \xi_2(0) \end{pmatrix} = \begin{pmatrix} 1 \\ 0 \end{pmatrix}, \qquad \begin{pmatrix} 0 \\ 1 \end{pmatrix}. \tag{14}$$

This set of independent initial conditions results in the transition matrix $\boldsymbol{\Phi}(p, 0)$ being equal to M.

Substituting equation (13) into equation (14) and equating terms of equal powers of ε leads to the zeroth order equation

$$\dot{\mathbf{x}} = A(t, 0)\mathbf{x}, \qquad \mathbf{x}(0) = \begin{pmatrix} 1 \\ 0 \end{pmatrix}, \qquad \begin{pmatrix} 0 \\ 1 \end{pmatrix}. \tag{15}$$

Solving equation (15), we obtain $\mathbf{x}^{1,0}(t, 0)$ and $\mathbf{x}^{0,1}(t, 0)$. The solution of the zeroth order equation appears as a forcing term in the first order equation, which can now be solved in closed form. The first order equation is

$$\dot{\mathbf{y}} = A(t, 0)\mathbf{y} + \left(\frac{\partial A(t, \varepsilon)}{\partial\varepsilon}\right)_{\varepsilon=0}\mathbf{x}^{i,j}(t, 0), \qquad \mathbf{y}(0) = \begin{pmatrix} 0 \\ 0 \end{pmatrix}, \quad i, j = 0, 1. \tag{16}$$

Because the initial values of equation (14) do not depend on ε, the initial values of the variational system are [0, 0].

The second order equation

$$\dot{\mathbf{z}} = A(t, 0)\mathbf{z} + 2\left(\frac{\partial A(t, \varepsilon)}{\partial\varepsilon}\right)_{\varepsilon=0}\mathbf{y}^{i,j}(t, 0), \qquad \mathbf{z}(0) = \begin{pmatrix} 0 \\ 0 \end{pmatrix}, \quad i, j = 1, 0, \tag{17}$$

can be solved in a similar fashion.

We now have a Taylor series solution which includes terms up to the second order (equation (13)). The M period-advance map is given by the equation:

$$M = \begin{bmatrix} \xi_1^{1,0}(p, \varepsilon) & \xi_1^{0,1}(p, \varepsilon) \\ \xi_2^{1,0}(p, \varepsilon) & \xi_2^{0,1}(p, \varepsilon) \end{bmatrix}, \qquad p = 2\pi/\omega. \tag{18}$$

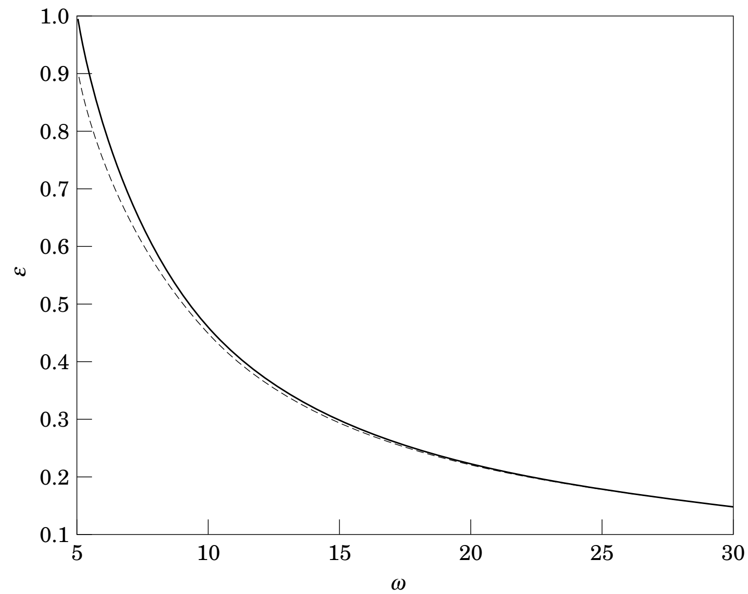

Figure 2. The stability border: - - - -, solution of Landau and Lifshitz; —, solution by the proposed technique.

Tr (M) is used to determine the stability border (equation (12)), which leads to the equation

$$|\xi_1^{1,0}(p, \varepsilon) + \xi_2^{0,1}(p, \varepsilon)| = 2. \tag{19}$$

The closed form solution of the inverted pendulum was determined using a symbolic manipulator, which resulted in the expression

$$\left| \mathrm{e}^{-2\sqrt{g}\pi/\sqrt{l}\omega} + \mathrm{e}^{2\sqrt{g}\pi/\sqrt{l}\omega} + \frac{(1 - \mathrm{e}^{4\sqrt{g}\pi/\sqrt{l}\omega})\varepsilon^2\omega^3\pi}{\mathrm{e}^{2\sqrt{g}\pi/\sqrt{l}\omega}\sqrt{g}\sqrt{l}(4g + l\omega^2)} \right| = 2. \tag{20}$$

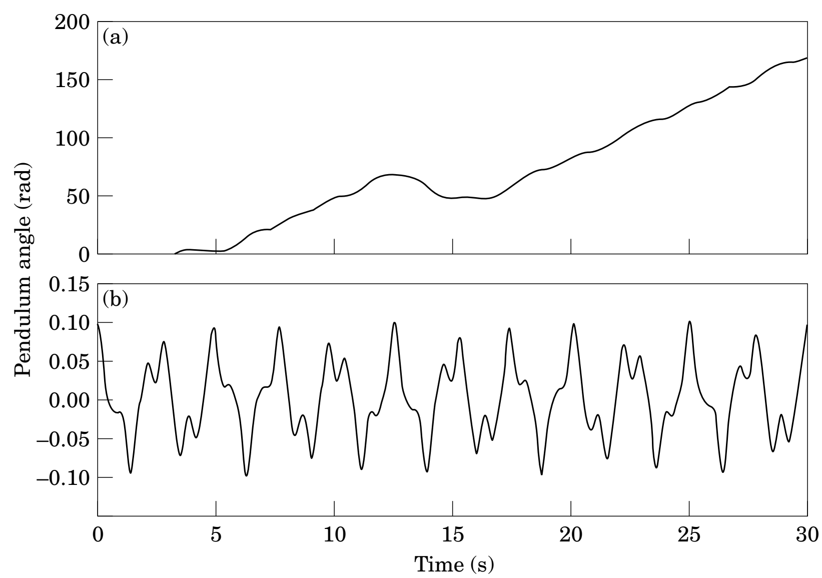

Figure 3. Numerical simulation: (a) $\omega = 9$, $\varepsilon = 0{\cdot}5$; (b) $\omega = 9$, $\varepsilon = 0{\cdot}6$.

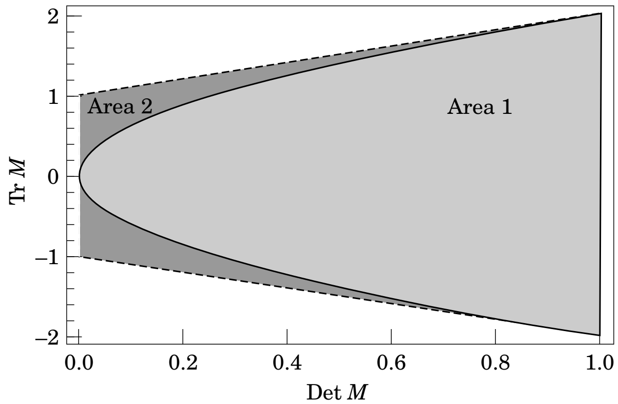

Figure 4. Stable areas for the damped case.

Solving equation (20) for ε, we have

$$\varepsilon(\omega) = \frac{g^{1/4} l^{1/4} \sqrt{-2l + 2\,\mathrm{e}^{2\sqrt{g}\pi/\sqrt{l}\omega} l - (8g/\omega^2) + \dfrac{8\,\mathrm{e}^{2\sqrt{g}\pi/\sqrt{l}\omega} g}{\omega^2}}}{\sqrt{1 + e^{2\sqrt{g}\pi/\sqrt{l}\omega}}\sqrt{\omega}\sqrt{\pi}}. \quad (21)$$

Landau and Lifshitz [2] solved for the stability border of an undamped inverted pendulum using the average technique, which resulted in the equation

$$\omega^2 \varepsilon^2 - 2gl = 0. \quad (22)$$

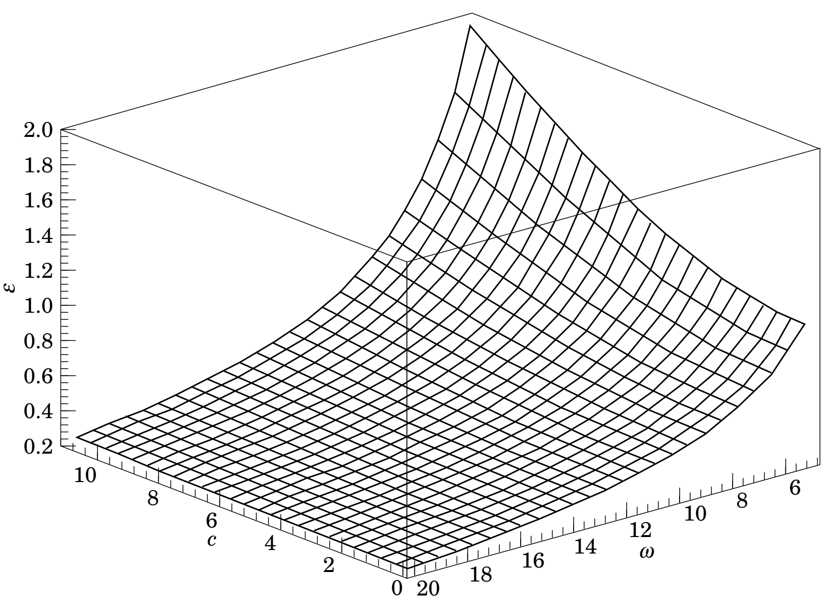

Figure 5. The stability surface.

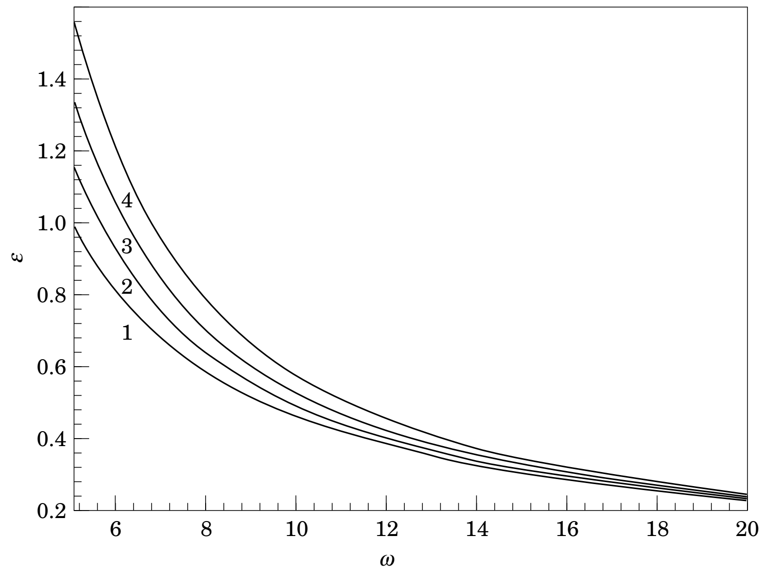

Figure 6. Stability contours: 1, $c = 0$; 2, $c = 4$; 3, $c = 6$; 4, $c = 8$.

The stability borders resulting from equations (21) and (22), which tend to merge with each other with increasing forcing frequency, are illustrated in Figure 2. Any combination of forcing amplitude and frequency that lies above the curves should result in the vertically upright position of the pendulum being a stable equilbrium position. For a forcing frequency of 9 rad/s, equation (21) requires the forcing amplitude to be greater than 0·512 for stability and equation (22) requires the forcing amplitude to be greater than 0·492. Thus, the two equations predict different characteristics for an forcing amplitude of 0·5. Numerical simulation of the non-linear undamped system for a forcing amplitude of 0·5 (Figure 3(a)), illustrates that the system is unstable, exemplifying that the stability border

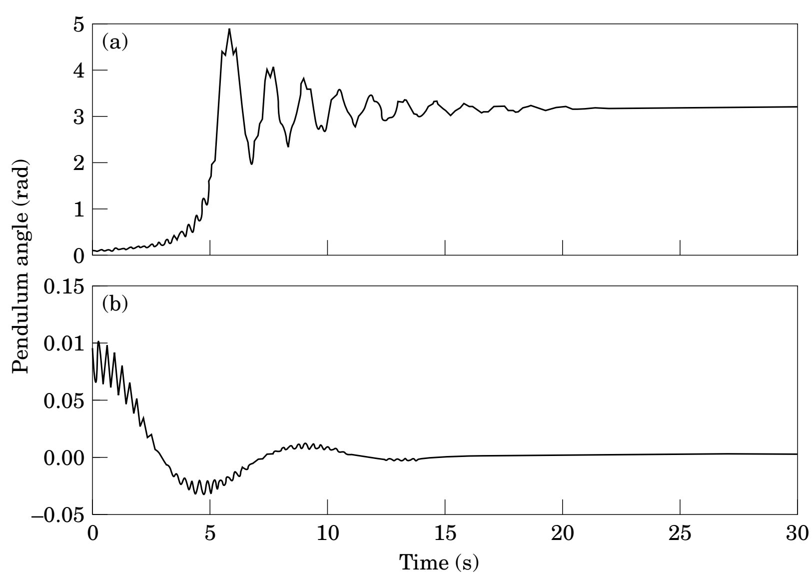

Figure 7. Numerical simulation: (a) $\omega = 20$, $\varepsilon = 0{\cdot}22$; (b) $\omega = 20$, $\varepsilon = 0{\cdot}23$.

estimated by the proposed approach is more accurate than that estimated by equation (22). The expected stability of the equilibrium point for a forcing amplitude of 0·6 is confirmed in Figure 3(b). Figure 3(b) reveals the existence of a high frequency signal which corresponds to the frequency of excitation, superposed on a low frequency signal.

3. PARAMETRICALLY EXCITED DAMPED INVERTED PENDULUM

In this section we investigate the stability of the inverted pendulum which is subject to viscous damping at the pivot. The dynamics of the damped inverted pendulum are given by the state space equation

$$\begin{pmatrix} \dot{x}_1 \\ \dot{x}_2 \end{pmatrix} = \begin{bmatrix} 0 & 1 \\ \dfrac{g}{l} - \dfrac{\varepsilon\omega_2}{l}\cos(\omega t) & -c \end{bmatrix} \begin{pmatrix} x_1 \\ x_2 \end{pmatrix}, \tag{23}$$

Equation (23) has the same form as equation (4) with a period $p = 2\pi/\omega$. The procedure to establish the stability boundary is identical to the one used for the undamped system. The only difference is that $\mathrm{Tr}\,(A) \neq 0$, which results in constraints that are different from the undamped case to determine stability. From equations (6), (7) and (23) it follows that $\mathrm{Det}\,(M) = \mathrm{e}^{\int_0^p - c\,\mathrm{d}\tau} = \mathrm{e}^{-cp}$, where c is the damping coefficient and $c \geqslant 0$. With the knowledge that the stability of the upright position of the pendulum depends on the absolute values of the characteristic roots of the *period-advance* map $M = g_0^p$, we substitute $\mathrm{Det}\,(M)$ into equation (5), resulting in the characteristic equation of the M matrix,

$$\sigma^2 - \mathrm{Tr}\,(M)\sigma + \mathrm{e}^{-cp} = 0, \tag{24}$$

the roots of which are

$$\sigma_{1,2} = \frac{\mathrm{Tr}\,(M) \pm \sqrt{\mathrm{Tr}^2\,(M) - 4\,\mathrm{Det}\,(M)}}{2}. \tag{25}$$

We investigate, separately, the real and the complex roots cases. It is evident that

$$|\mathrm{Tr}\,(M)| < 2\sqrt{\mathrm{Det}\,(M)} \Rightarrow \sigma_1, \sigma_2 \in \mathscr{C}, \qquad |\mathrm{Tr}\,(M)| \geqslant 2\sqrt{\mathrm{Det}\,(M)} \Rightarrow \sigma_1, \sigma_2 \in \Re. \tag{26,27}$$

In the complex case, $\mathrm{Det}\,(M) = \mathrm{e}^{-cp}$ is smaller than 1, since c and p are positive numbers. This implies stability, since the product of the roots is less than 1.

In the real case the necessary conditions for stability are satisfied if

$$\frac{\mathrm{Tr}\,(M) - \sqrt{\mathrm{Tr}^2\,(M) - 4\,\mathrm{Det}\,(M)}}{2} \geqslant -1, \qquad \frac{\mathrm{Tr}\,(M) + \sqrt{\mathrm{Tr}^2\,(M) - 4\,\mathrm{Det}\,(M)}}{2} \leqslant 1. \tag{28}$$

Combining the stability constraints for the two cases, we have, from equations (26) and (28),

$$\begin{cases} -2\,\mathrm{e}^{-cp/2} < \mathrm{Tr}\,(M) < 2\,\mathrm{e}^{-cp/2}, & \text{if } |\mathrm{Tr}\,(M)| < 2\sqrt{\mathrm{Det}\,(M)} \\ -1 - \mathrm{Det}\,(M) \leqslant \mathrm{Tr}\,(M) \leqslant 1 + \mathrm{Det}\,(M), & \text{if } |\mathrm{Tr}\,(M)| \geqslant 2\sqrt{\mathrm{Det}\,(M)} \end{cases}. \tag{29}$$

From equation (29), the stable area is given by the inequality

$$|\mathrm{Tr}\,(M)| \leqslant 1 + \mathrm{e}^{-cp}, \tag{30}$$

which is illustrated in Figure 4. Area 1 corresponds to equation (26) and area 2 corresponds to equation (28).

The calculation of Tr (M) or, to be specific, the second order approximation of Tr (M), is carried out in the same fashion as the undamped case using variational systems. The difference is the calculation of the stability border, which is based on equation (30). Therefore, the stability border is a function of ε, ω, l and c. In the interest of brevity, the closed form expression representing the stability border is not included here.

The surface that represents the stability border for the damped system is illustrated in Figure 5. Any combination of the damping constant, amplitude and frequency that lie above the surface leads to the upright position being a stable equilibrium point. It can be seen from the graph that the stability is a strong function of the damping constant. Thus, for larger damping a larger amplitude of forcing is required to stabilize the system compared to a system with low damping, for the same forcing frequency. The variation of the stability boundary for different values of the damping constant is demonstrated in Figure 6. This figure clearly shows that for given forcing frequency, the forcing amplitude increases with damping, for stability.

The system response for a forcing frequency of 20 rad/s and forcing amplitudes of 0·22 and 0·23 is illustrated in Figure 7. The stability surface indicates that the forcing amplitude corresponding to a damping constant of 0·5 and a forcing frequency of 20 is 0·2234. For a forcing amplitude of 0·22, the system settles to the equilibrium position that corresponds to the vertically down postion and the forcing amplitude of 0·23 forces the system to come to rest at the vertically upright position. Thus, it is evident that the proposed approach to arrive at the stability surface is fairly accurate.

4. CONCLUSIONS

A perturbation approach has been used to arrive at a closed form solution of the stability surface for a damped inverted pendulum. A recursive solution is used to arrive at the period-advance map, the eigenvalues of which determine the stability of the system. The stability border illustrates that, for high frequencies, the system is not a strong function of the damping in the system. However, at larger damping, the amplitude of forcing for a given frequency increases significantly, compared to the undamped case. Numerical simulations of the non-linear system are used to corroborate that the stability border predicted by the linearized approximation is reliable. The solution for the undamped case, which is a special case of the damped system, has been shown to closely approach that determined by Landau and Lifshitz [2].

REFERENCES

1. A. STEPHENSON 1908 *Philosophical Magazine* **15**, 233–237. On induced stability.
2. L. D. LANDAU and E. M. LIFSHITZ 1960 *Mechanics*. Oxford: Pergamon Press.
3. M. J. CLIFFORD and S. R. BISHOP 1994 *Journal of Sound and Vibration* **174**, 572–576. Approximating the escape zone for the parametrically excited pendulum.
4. D. CAPECCHI and S. R. BISHOP 1994 *International Journal for the Dynamics and Stability of Systems* **9**, 123–143. Periodic oscillations and attracting basins for a parametrically excited pendulum.
5. D. J. ACHESON 1993 *Proceedings of the Royal Society London* **443**, 239–245. A pendulum theorem.
6. C. S. HSU 1975 *Transactions of the American Society of Mechanical Engineers*, *Journal of Applied Mechanics* **42**, 176–182. Limit cycle oscillations of parametrically excited second-order nonlinear systems.
7. V. I. ARNOLD 1973 *Ordinary Differential Equations*. Translated and edited by Richard A. Silverman. Cambridge: MIT Press.
8. D. L. LUKES 1982 *Differential Equations*: *Classical to Controlled*. New York: Academic Press.
9. L. S. Pontriagin 1962 *Ordinary Differential Equations* Reading, MA: Addison-Wesley.